27 May 2010, 4:30 pm - 6:20 pm

A Probabilistic Method for the Prediction of Earthquake-Induced Slope Displacements

Simone Barani
University of Genoa, Italy

Paolo Bazzurro
AIR Worldwide Co., San Francisco, CA

Fabrizio Pelli
Geodeco S.p.A., Italy

Fifth International Conference on
Recent Advances in Geotechnical Earthquake Engineering and Soil Dynamics
and Symposium in Honor of Professor I.M. Idriss
May 24-29, 2010 • San Diego, California

A PROBABILISTIC METHOD FOR THE PREDICTION OF EARTHQUAKE-INDUCED SLOPE DISPLACEMENTS

Simone Barani
Dip.Te.Ris.
University of Genoa
Viale Benedetto XV
16132 Genoa, Italy

Paolo Bazzurro
AIR Worldwide Co.
San Francisco, CA, USA

Fabrizio Pelli
Geodeco S.p.A.
Via Aurelia 24
16031 Genoa, Italy

ABSTRACT

This work presents a probabilistic method for estimating earthquake-induced nonlinear slope displacements. This method is applicable to any kind of slope, embankment and earth/rockfill dam. When coupled with Probabilistic Seismic Hazard Analysis at the slope site, it produces estimates of the annual probability that a permanent deformation of the slope will be exceeded. The proposed method uses a set of 2D numerical analyses with non-linear constitutive relationships for the soil formations to establish a probabilistic relationship between one or more ground motion parameters and the permanent displacement at a specific location within the slope. The analyses, which are performed using the computer code FLAC 5.0 (Itasca, 2005), use as input a set of different recorded accelerograms that include both horizontal and vertical components. The method is applied to the Salcito landslide (Molise, Southern Italy), which was investigated in detail by Bozzano et al. (2008). The stability of the same slope is also assessed using the conventional Newmark's method and a decoupled approach and the results are compared and contrasted with those obtained using FLAC.

INTRODUCTION

The evaluation of the seismic performance of earth/rockfill dams, solid-waste landfills, and natural slopes is recognized as one of the most important activities of the geotechnical earthquake engineering since failures can produce significant economic and human losses. In particular, the stability of slopes subjected to seismic action is of primary importance since, in many cases, landslides are responsible for a significant proportion of total earthquake damage. Thus, predicting slope performance during earthquakes is often essential for design, urban planning, and for seismic hazard studies.

Seismic slope performance for any given input ground motion can be assessed in different ways, ranging from simple pseudo-static procedures, which consider the seismic shaking as an additional force, to advanced non-linear dynamic analyses. Nowadays, the Newmark (1965) sliding-block method is still the most widely used procedure for evaluating earthquake-induced slope displacements (e.g., Miles_and_Ho, 1999; Barani et al., 2007). This method simplifies a potential failure mass as a rigid-block resisting on an inclined plane. The block starts moving relative to the plane when the total driving force down slope exceeds the yield resistance of the slip surface. The block velocity increases until the earthquake-induced acceleration become lower than a critical value (critical acceleration), then the block is decelerated by the friction force acting on its base, and its velocity progressively decreases to zero. The permanent displacement of the sliding mass can be calculated by integrating the relative velocity during slippage as a function of time or, in other words, by double-integrating the parts of the corresponding accelerogram that exceed the critical acceleration. The main advantage of Newmark's method is its theoretical and practical simplicity. However, it presents some limitations that are the result of several simplifying assumptions (Wartman et al., 2003). Chief among these assumptions is that of soil rigidity. Indeed, the landslide mass is assumed to behave in a rigid, perfectly plastic manner. "*This assumption is reasonable for relatively thin landslides in stiff or brittle materials, but it introduces significant errors as landslides become thicker and material becomes softer*" (Jibson and Jibson, 2003). Thus, a number of modifications to the original Newmark approach and more sophisticated methods have been proposed during the last three decades in order to achieve more accurate displacement estimates. In particular, Makdisi and Seed (1978) proposed a decoupled procedure that, contrary to the Newmark rigid-block approach, accounts for the dynamic response of the sliding mass. First, a dynamic analysis of the slope is performed assuming that no relative displacement occurs along the failure surface. Then, the acceleration time history from the dynamic analysis is used as the input in a rigid-block calculation to estimate the slope displacement. Five years later, Lin and Whitman (1983) pointed out that a decoupled analysis may not be very effective since it does not account for the effects of slip on the ground motion. Thus, they suggested the application of a coupled procedure in which the dynamic response of the sliding mass and the permanent displacement are modeled together. In recent years, moreover, simplified procedures based on empirical slope displacement predictive relations have been proposed (e.g., Jibson, 1993; Bray et al., 1998; Romeo, 2000; Bray and Travasarou, 2007). A critical and detailed review of simplified and sophisticated methods can be found in the articles of Jibson (1993), Rathje and Bray (2000), and, Bray (2007).

In the work presented here 2D numerical analyses are performed to derive an empirical relation for the prediction of soil displacement as a function of one or more ground motion parameters. This soil response function can then be coupled with Probabilistic Seismic Hazard Analysis (PSHA) at the bedrock to establish the annual rate of exceedance of permanent slope deformation of different severity (Bazzurro et al., 1994; Rathje and Saygili, 2008). If more than one ground motion parameter is deemed necessary for an accurate soil response prediction, then the scalar PSHA can be replaced by its vectorized version VPSHA (Bazzurro and Cornell, 2002) to establish the joint hazard at the slope site. Thus, this probabilistic approach to estimate seismically induced displacements refines the methodology presented by Bazzurro et al. (1994) on the same topic and represents an extension of that by Bazzurro and Cornell (2004a and 2004b) for 1D site amplification assessment in non linear soils. The numerical analyses to establish the correlation between ground motion parameters and soil displacement is performed for the case study of the Salcito landslide (Bozzano et al., 2008) using the computer code FLAC 5.0 (Itasca, 2005). The uncertainty in ground motion time histories is considered by using a set of different recorded accelerograms that include both horizontal and vertical components. Finally, results are compared with those obtained from decoupled and standard rigid-block analyses for the same suite of ground motions.

SALCITO LANDSLIDE

The Salcito landslide is located in the northern part of the Molise Region (Southern Italy), an area characterized by a low seismic activity (Fig. 1). Although local earthquakes are rare and usually fairly weak, this area may be affected by stronger events originating from seismic sources located further north and south at relatively large distances from the site. This phenomenon is confirmed by macroseismic data (e.g., Macroseismic Database of Italy 2004 – DBMI04, Stucchi et al., 2007) documenting the effects of strong, distant earthquakes which occurred in the past (e.g., July 26, 1805 Bojano earthquake with moment magnitude $M_w = 6.6$).

The Salcito landslide was re-activated following the Molise earthquake ($M_w = 5.8$), which occurred on October 31, 2002 killing 30 people due to the collapse of a primary school in San Giuliano di Puglia. A detailed study by Bozzano et al. (2008) associates the landslide re-activation to self-excitation processes related to 1D and 2D local amplification effects. The former are ascribed to the response of the landslide mass in the 2-3 Hz frequency range, while the latter can be related to a complex basin-like structure responsible for ground motion amplification at approximately 1 Hz.

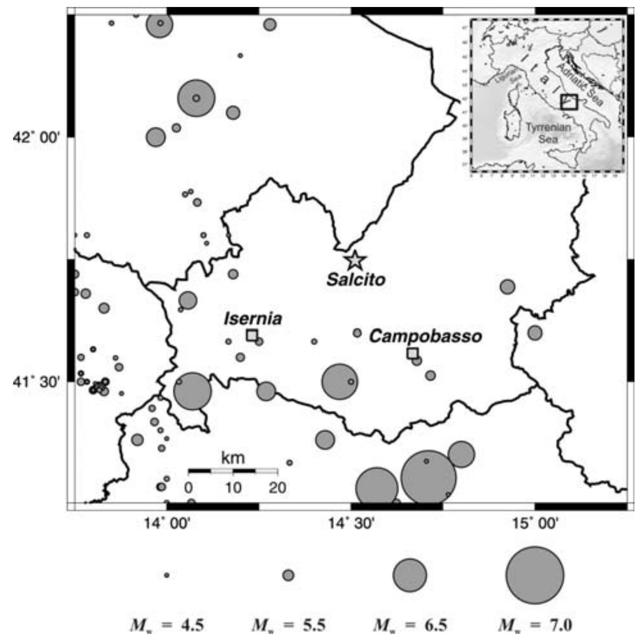

Fig. 1. Distribution of seismicity based on the CPTI04 catalogue (Gruppo di Lavoro CPTI, 2004).

The Salcito landslide has developed within the Argille Varicolori formation, which consists of fissured clay shales with local intensely-sheared arenaceous and marly limestone beds (Fig. 2a). The landslide mobilized about 20 to 40 Mm^3 of clays overlying marls and calcarenites belonging to the Tufillo formation with displacements of some tens of decimeters (Bozzano et al., 2004). The mass movements occurred mainly on a planar surface about 50 m deep (Bianchi Fasani et al., 2004), next to the bedrock. Secondary sliding surfaces were also observed within the landslide mass at shallower depths. When the reactivation took place, most of the sliding mass was below the ground water level, which was about 1 m below the ground surface (Bozzano et al., 2004).

LANDSLIDE MODELING AND RESPONSE ANALYSES

In order to establish correlations between ground motion parameters and soil displacements, dynamic non-linear analyses were performed using the computer code FLAC 5.0 (Itasca, 2005). Similarly to Bozzano et al. (2008), the numerical model adopted in this study simulates an infinite slope characterized by three layers with different material properties (Fig. 2b).

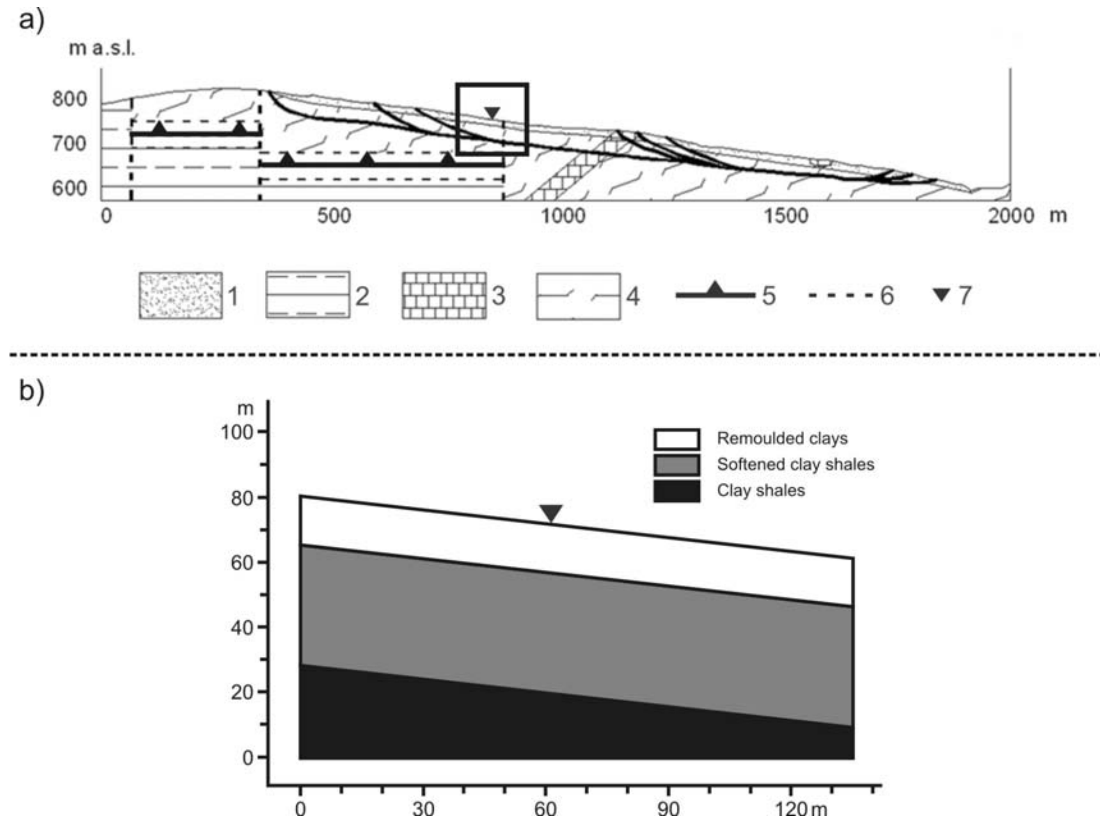

Fig. 2.Geological section of the Salcito landslide(after Bozzano et al., 2008) (a) and numerical model used in the analyses (b). In Figure (a): 1, landslide mass; 2, marls with calcarenites (Tufillo Formation); 3, calcarenites and marls of the Sannio Unit; 4, fissured clay shales (Argille Varicolori Formation of the Molise Unit); 5, thrust; 6, tear fault; 7, location in the numerical model where the displacements are calculated; the square area indicates the section modeled; a.s.l.: above sea level.

The soil and rock cyclic energy dissipation is considered by using specific strain-dependent modulus and damping functions. Specifically, for the soil layers overlaying the bedrock, hysteretic damping is modeled based on the shear modulus reduction curves published by Bozzano et al. (2008). On the other hand, the shear-modulus reduction curve for rock included in sample data files for the original Shake program (Schnabel et al., 1972) was adopted for the rock-like clay shale, for which specific information is not available. The hysteretic model is coupled with the Mohr-Coulomb failure criterion, assuming a zero dilatancy non-associated flow rule and adopting an effective stress approach. A small amount of mass- and stiffness-proportional Rayleigh damping was also applied, and a value of 1.0% with a central frequency of 1.0 Hz was assigned to all materials. The geotechnical properties assigned to each layer are summarized in Table 1.

The model consists of about 9,000 zones with variable size, designed with consideration to the frequency content of the input records in relation with the shear wave velocity characterizing each material. The criterion proposed by Kuhlemeyer and Lysmer (1973) was applied to establish the maximum zone size compatible with accurate modeling of wave propagation through the geologic media, and zones smaller than approximately 1/10 to 1/8 of the wavelength associated with the highest frequency component of the input motion were selected. Hence, an element size of 1 m was used for the shallowest soil layers, whereas a size of 2 m was adopted in the bedrock (i.e., clay shales). According to this approach the model allows effective propagation of waves with frequencies up to 16 Hz, which is adequate to transmit to the ground surface most of the energy content of the input time histories.

Table 1. Material properties (after Bozzano et al., 2008): h, soil thickness; G_{max}, shear modulus; K, bulk modulus; ρ, dry density; n, porosity; k_m, mobility coefficient; φ, friction angle; c, cohesion; t, tension cutoff.

Material	***h* (m)**	**G_{max} (Pa)**	***K* (Pa)**	**ρ (kg/m^3)**	***n***	**k_m (m^2/Pa·s)**	**φ (°)**	***c* (Pa)**	***t* (Pa)**
Remoulded clays	15	4.79E+07	7.98E+07	1750	0.35	1.02E-12	17	0	0
Softened clay shales	35	2.20E+08	3.67E+08	1750	0.35	1.02E-12	17	0	0
Shear zone	2	2.20E+08	3.67E+08	1750	0.35	1.02E-15	17	0	0
Clay shales	-	2.16E+09	3.59E+09	1900	0.30	1.02E-13	22	2.30E+04	5.70E+04

Table 2. List of ground motion records used in numerical simulations. M_w is for moment magnitude, R for epicentral distance, and PHA and PVA indicate peak horizontal and vertical acceleration, respectively.

Earthquake #	Earquake Name	Earthquake Country	Date	Epicentre Lat	Epicentre Lon	M_w	R (km)	Station Code	PHA (g)	PVA (g)	Databank
1	Friuli (4th shock)	Italy	15/09/1976	46.30	13.18	6.0	16.4	SRC0	0.2490	0.0870	ITACA
2	Friuli	Italy	16/09/1977	46.28	12.98	5.4	9.1	SMU	0.1809	0.0529	ITACA
3	Patti Gulf	Italy	15/04/1978	38.27	15.11	5.5	33.0	NAS	0.1494	0.0817	ITACA
4	Montenegro	Serbia & Montenegro	15/04/1979	41.98	18.98	6.9	105.0	DUB	0.2559	0.2085	ESD
5	Montenegro	Serbia & Montenegro	15/04/1979	41.98	18.98	6.9	65.0	HRZ	0.0749	0.0256	ESD
6	Irpinia	Italy	23/11/1980	40.81	15.34	6.9	77.2	B-AUL	0.0423	0.0193	PEER
7	-	Italy	16/01/1981	40.84	10.50	4.8	12.1	CR3	0.1693	0.0449	ITACA
8	Campano Lucano (aftershock)	Italy	14/02/1981	41.00	14.67	5.1	17.0	ARN	0.0293	0.0183	ESD
9	-	Italy	18/09/1982	38.37	14.97	3.9	32.7	NAS	0.0793	0.0414	ITACA
10	Garfagnana	Italy	23/01/1985	44.06	10.41	4.5	3.7	BRG	0.0432	0.0193	ITACA
11	Loma Prieta	California	18/10/1989	37.04	-121.88	6.9	28.6	G01	0.4731	0.2088	PEER
12	Firuzabad	Iran	20/06/1994	29.01	52.64	5.9	21.0	ZRT	0.3104	0.1091	ESD
13	Kozani	Greece	13/05/1995	40.18	21.66	6.5	17.0	KOZ	0.2079	0.0832	ESD
14	Umbria-Marche	Italy	26/09/1997	43.02	12.89	5.6	35.2	CSC	0.0296	0.0174	ITACA
15	Izmit (aftershock)	Turkey	07/11/1999	40.70	30.72	4.9	14.0	C0375	0.3517	0.0706	ESD
16	South Iceland (aftershock)	Iceland	17/06/2000	63.97	-20.36	6.5	5.0	106	0.3376	0.2734	ESD
17	-	Tōhoku (offshore)	05/12/2002	38.72	142.26	4.9	80.7	MYG	0.2590	0.0674	K-NET
18	Bingol	Turkey	01/05/2003	39.01	40.51	6.3	14.0	BIN	0.5151	0.4514	ESD
19	Olfus	Iceland	29/05/2008	64.01	-21.01	6.3	8.0	101	0.5363	0.2516	ESD
20	L'Aquila	Italy	06/04/2009	42.33	13.33	6.3	31.6	ORC	0.0909	0.0449	ITACA

Prior to the dynamic simulations, a static analysis was carried out to establish the initial effective stress field throughout the model, and a stationary ground flow analysis was performed to establish the pore pressure distribution.

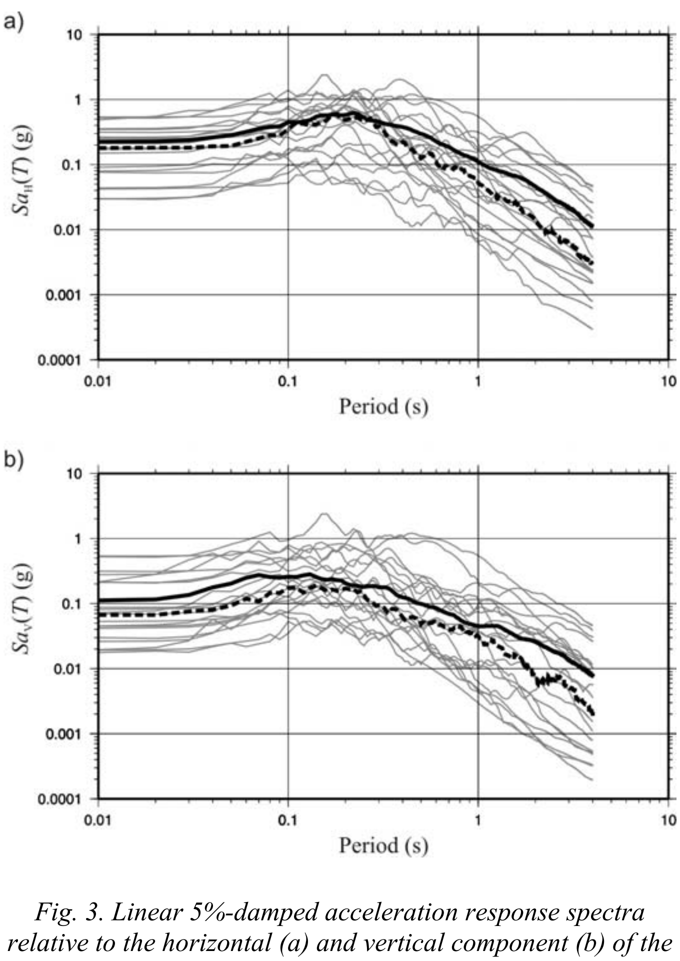

Fig. 3. Linear 5%-damped acceleration response spectra relative to the horizontal (a) and vertical component (b) of the records selected for numerical analyses. Solid and dashed lines indicate the average and median spectra, respectively.

In order to minimize reflection of outward propagating waves back into the grid, an absorbing boundary was applied along the base of the model, whereas free-field type boundaries (Cundall et al., 1980) were applied along the sides. The quiet-boundary scheme adopted in FLAC, proposed by Lysmer and Kuhlemeyer (1969) is based on dashpots attached independently in the normal and shear directions.

The seismic input applied along the base of the model consists of a set of 20 real acceleration time histories from 40 worldwide weak and strong earthquakes recorded at sites classified as "rock" (Table 2). Here, the term "rock" refers to sites with average shear wave velocity in the upper 30 m ($V_{S,30}$) greater than 800 m/s, accordingly to the classification proposed by the Eurocode 8 (Comitè Europèen de Normalisation – CEN, 2003) and by the Italian building code (Ministero delle Infrastrutture e dei Trasporti, 2008). For each event, both the horizontal component with the highest peak ground acceleration (PHA) value and the vertical component were applied at the base of the model. Further information and criteria adopted in record selection can be found in the article by Barani et al. (2010) submitted for publication in the proceedings of this conference. The 5%-damped acceleration response spectra of the selected records are shown in Fig. 3.

Prior to apply the selected time histories (target motions), the appropriate dynamic loading for the base of the model needs to be determined. First, a 16 Hz Butterworth low-pass filter was applied to all records. The low-pass frequency, compatible with the zone size, was chosen after analyzing the frequency content (Fourier analysis) of the selected accelerograms. Then, the appropriate input motion for FLAC is estimated by applying a 0.5 factor to the time history recorded at the ground surface (Mejia and Dawson, 2006) in order to obtain the corresponding deconvolved upward propagating motion. Due to the quiet boundary, it was not possible to apply directly velocity or acceleration records at the model bottom. Therefore, the accelerograms were integrated to obtain velocity time histories that, in turn, were converted into stress waves using the following relationships:

$$\sigma_n = 2\rho C_P v_n \tag{1}$$

$$\sigma_s = 2\rho C_S v_s \tag{2}$$

where σ_n and σ_s are the applied normal and shear stresses, respectively, ρ is the material density, C_P and C_S are the P- and S-wave velocities, respectively, and v_n and v_s are the input normal and shear particle velocities.

The factor of two in Eqs. 1 and 2 accounts for the fact that the amplitude of the applied stress waves must be doubled to keep into account that half the input energy is absorbed by the viscous boundary. However, some adjustments are required to obtain input motions consistent with the target motions at the outcrop. To this end, stress histories were propagated through a 1D model consisting of one single layer of saturated clay shales (i.e., bedrock) and the PHA of the surface accelerograms was then compared with that of the corrsponding target motions. Correction factors, defined as the ratio of the surface PHA from 1D simulations to the target PHA value, were then applied to the stress histories derived by applying Eqs. 1 and 2.

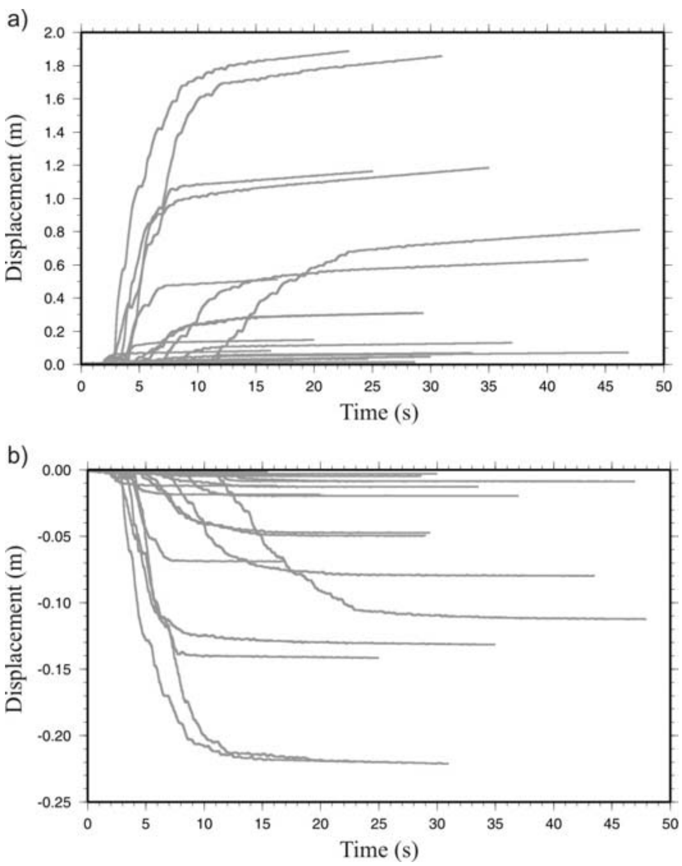

Fig. 4. Horizontal (a) and vertical (b) components of displacement as derived from response analyses.

Results of 2D dynamic analyses are presented in Fig. 4 where displacement histories in both the horizontal and vertical directions are shown. It should be observed that, although the element size was calibrated for wave propagation up to 16 Hz and target time histories were processed for baseline correction, accelerograms recorded at the base of the model contain spurious nonphysical "ringing" (superimposed oscillations with frequencies generally greater than 80-100 Hz) and exhibit some limited residual displacements. In order to evaluate the effects of these spurious frequencies on the output displacements provided by FLAC, surface accelerograms were low-pass filtered at 16 Hz and double integrated to obtain alternative displacement values that were compared with those calculated by FLAC. It was found that the effects of the spurious frequencies on displacements is small, and can therefore be neglected.

PREDICTION OF SOIL DISPLACEMENT

Empirical relations for the prediction of soil displacement as a function of period-independent and period-dependent ground motion parameters are derived through regression analyses. Specifically, the permanent displacement calculated along the slope direction, D, is related to the pseudo-velocity response spectrum intensity (Housner, 1952), SI_H, Arias intensity (Arias, 1970), Ia_H, 5%-damped horizontal and vertical spectral acceleration at given spectral periods, $Sa_H(T)$ and $Sa_V(T)$, spectral acceleration at the initial fundamental soil period, $Sa_H(T_S)$, and spectral acceleration at a degraded period equal to 1.5 times T_S ($T_S \approx 0.76$ s). Subscripts H and V in our notation refer to the horizontal and vertical component of motion, respectively.

The Arias intensity is calculated by integration over the duration of an accelerogram $a(t)$ (Arias, 1970):

$$Ia = \frac{\pi}{2g} \int_0^{T_d} a(t)^2 \, dt \tag{3}$$

where g is the acceleration of gravity and T_d is the duration of the ground shaking.

The pseudo-velocity response spectrum intensity (or Housner intensity) is calculated as (Housner, 1952):

$$SI = \int_{0.1}^{2.5} PSV(T) dT \tag{4}$$

where $PSV(T)$ indicates the 5%-damped pseudo-velocity response spectrum.

Previous works by other authors (e.g., Jibson, 1993; Harp and Wilson, 1995) pointed out that integral ground motion parameters, such as the Arias intensity and Housner intensity, correlate better with landslide displacement than parameters associated with a single period. Following previous definitions, indeed, Ia and SI are more comprehensive and quantitative measures of the ground shaking than PGA and spectral acceleration as they account for the amplitude and frequency content of earthquakes in a single parameter. Specifically, Arias intensity was found to be the most efficient intensity measure for stiff and weak slopes while response spectrum intensity is preferable for flexible slopes (Bray, 2007). The use of this latter parameter was also suggested by Makdisi and Seed (1978) for evaluation of the response of earth structures with T_S between 0.6 and 2.0 s.

First, empirical relations between D and period-independent parameters are established. The (log-) regression model adopted is represented by the following general equation:

$$\ln D = c_1 + c_2 \ln X + \varepsilon \tag{5}$$

where X is the predictor (i.e., SI_H or Ia_H), and ε is the Gaussian residual with zero mean and standard deviation, $\sigma_{\ln(D)}$. An estimate of $\sigma_{\ln(D)}$ is obtained via statistical regression. Note that $\sigma_{\ln(D)}$ is conditional on X but the conditioning has been dropped from the notation for simplicity.

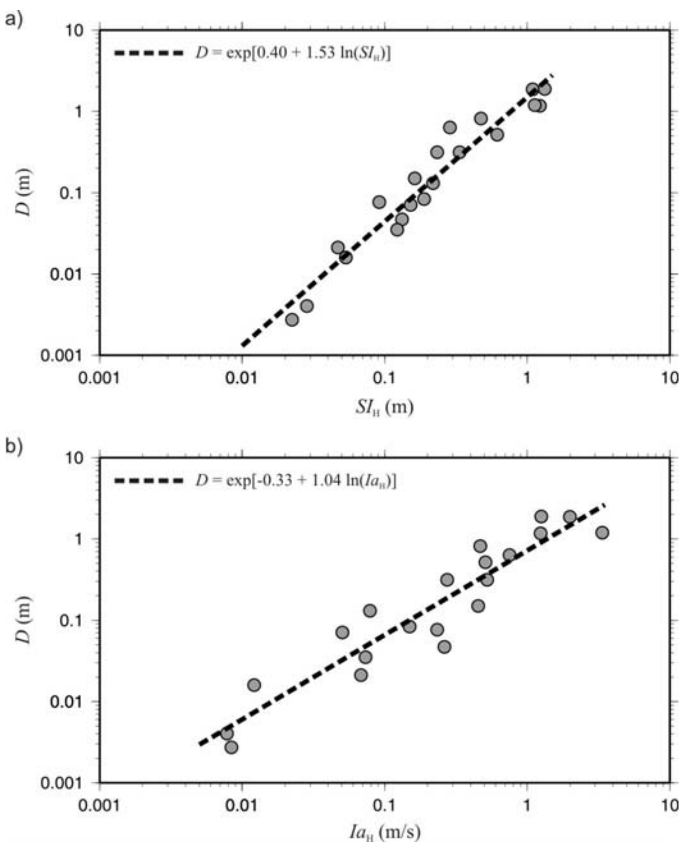

Fig. 5. Regressions of residual displacement on horizontal Housner intensity (a) and horizontal Arias intensity (b) .

Results from single regressions are shown in Fig. 5 where the distributions of D versus SI_H (Fig. 5a) and Ia_H (Fig. 5b) are displayed. The figure shows a strong positive correlation between D and both the independent variables, as high displacement values are generated by high values of SI_H and Ia_H. Following Jibson (2007), multiple regression models are also examined, adding the term a_c/PHA (called critical acceleration ratio) to the simple models in SI_H and Ia_H. Here, $a_c = k_y g$ indicates the critical acceleration. The yield coefficient, k_y, was computed with reference to the shear surface located 15 m below ground level, by applying the following relationship, which keeps into account the effects of the groundwater seepage, parallel to the ground surface, on the factor of safety:

$$k_y = \frac{(\gamma_1 h_1 + (\gamma_2 - \gamma_w) h_2)\cos^2\beta \tan\varphi - (\gamma_1 h_1 + \gamma_2 h_2)\sin\beta\cos\beta}{(\gamma_1 h_1 + \gamma_2 h_2)\cos\beta} \tag{6}$$

where γ_1, γ_2 and h_1, h_2 are the total unit weights and the thicknesses of the soil layers located above and below the ground water surface, respectively, γ_w is the unit weight of the ground water, φ and β (= 8°) are the soil internal friction angle and the slope angle, respectively.

Although the adopted soil constitutive relationships do not consider possible pore pressure build-up due to cyclic loading, the analyses carried out with FLAC identified some residual excess pore pressures associated with shear deformation that, although limited (i.e., between zero and 10% of the initial values, depending on the magnitude of the residual displacement) affects to some extent the k_y values and, as a consequence, the computed permanent displacements. While a detailed discussion on the physical relevance of this pore pressure increase goes beyond the scope of this paper, which concentrates on the description of the probabilistic methodology, the effects of this excess pore pressure was kept into account, obtaining k_y values variable between 0.014 and 0.021.

Figure 6 compares the goodness of fit statistics for the simple and multiple regression models. The goodness of fit is evaluated by analyzing the standard deviation of the residual, $\sigma_{\ln(D)}$, and the coefficient of multiple determination, R^2(adj), adjusted for its associated degrees of freedom. This latter parameter is a measure of the effectiveness of the model in predicting the dependent variable. This statistic can take on any positive value less than or equal to 1, with a value closer to 1 indicating a better fit. As shown in Fig. 6, adding the a_c/PHA term to the simple models does not significantly improve the prediction and produces R^2(adj) values almost equal to those obtained from the SI_H and Ia_H models. More precisely, slight but negligible improvements in the prediction of D can be observed only when this term is added to the model in SI_H. Indeed, this produces a value of $\sigma_{\ln(D)}$ (= 0.43) that is 12% lower than that obtained from single regression ($\sigma_{\ln(D)}$ = 0.49). Comparing the goodness of fit statistics of the regression model in SI_H with those of the model in Ia_H reveals that this latter parameter is less effective in predicting slope displacement, confirming observations by Bray (2007) about the use SI_H to characterize the response of flexible slopes.

The effectiveness of period-dependent ground motion parameters in predicting landslide displacement is also examined. Results are presented in Fig. 7, which shows the variation $\sigma_{\ln(D)}$ and R^2(adj) with spectral period for different regression models. The figure clearly indicates that neglecting the (log-) linear terms $Sa_H(T_S)$ or $Sa_H(1.5T_S)$, which carries implicitly information on the soil fundamental frequency, results in a less accurate prediction of D. Thus, $Sa_H(T_S)$ and $Sa_H(1.5T_S)$ explain a large part of the variability related to D in all the spectral range considered. In particular, the multiple model in both $Sa_H(T)$ and $Sa_H(T_S)$ is found to be more efficient than the one including $Sa_H(1.5T_S)$, indicating, contrary to what observed by Travasarou and Bray (2007), that in this specific application $Sa_H(T_S)$ is more informative than $Sa_H(1.5T_S)$.

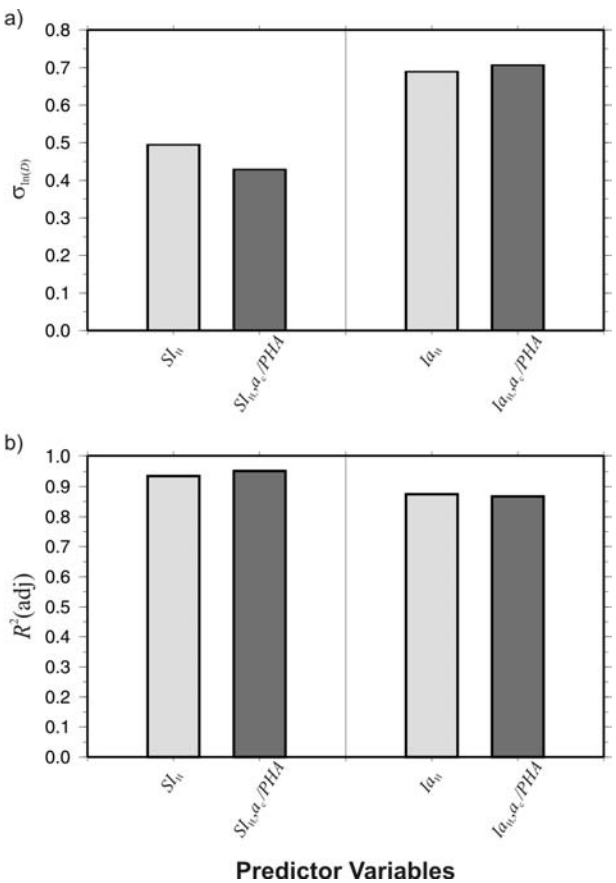

Fig. 6. Values of $\sigma_{ln(D)}$ (a) and R^2(adj) (b) obtained from single and multiple regressions of D on SI_H, Ia_H, and a_c/PHA.

Compared to the model in SI_H, the model in $Sa_H(T)$ and $Sa_H(T_S)$ is less effective in predicting slope displacement, when one uses $Sa_H(T)$ with T greater than 0.5s. However, the model that couples $Sa_H(T_S)$ with $Sa_H(T)$ at lower periods, especially in the neighborhood of 0.25 s, has a predictive power superior to that of the SI_H model. Note that this period is close to the resonant frequency of shallowest layer of the landslide mass (i.e. remoulded clays), approximately equal to 3.0-3.5 Hz (Bozzano et al., 2008), where the largest displacements are observed. Thus, following results from regression analyses, SI_H appears the single most helpful parameter in predicting slope displacement but, at least for this case study, a more efficient and accurate prediction can be obtained using a multiple regression model in both Sa(0.25s) and $Sa(T_S)$:

$$\ln D = 1.47 + 0.64 \ln Sa(0.25\text{s}) + 1.11 \ln Sa(T_S) \tag{7}$$

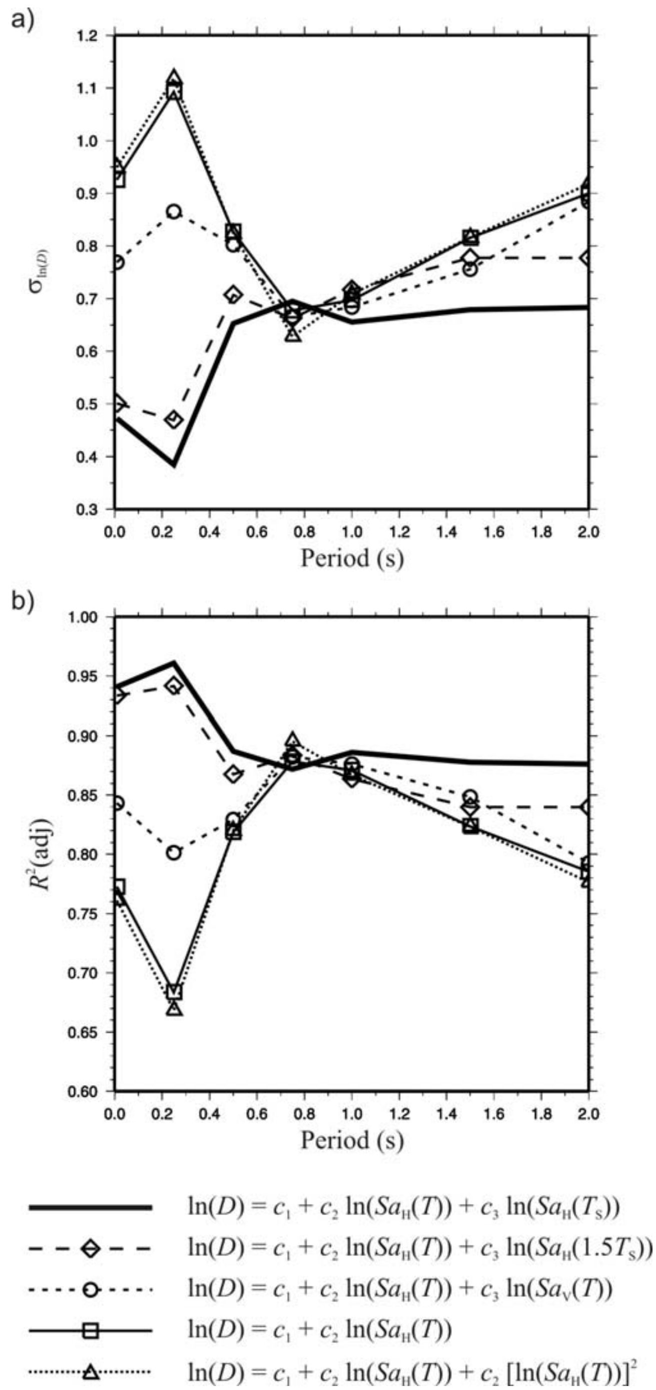

Fig. 7. Variation of $\sigma_{ln(D)}$ (a) and R^2(adj) (b) with spectral period for different regression models in $Sa_H(T)$.

COMPARISON WITH NEWMARK'S METHOD

Permanent displacements calculated using FLAC (coupled displacements hereinafter) are compared with those obtained using the conventional Newmark's rigid-block method and a decoupled approach for the same suite of ground motions. More specifically, only the horizontal component of each record in Table 2 was used as input in both the Newmark and decoupled analyses. In the former case (Newmark rigid-block analysis) the target acceleration time histories recorded on rock were adopted in the computation without considering site amplification, whereas in the latter (decoupled approach) the target time histories were first propagated to the ground surface through a 1D model representing the site stratigraphy (Table 1). The surface outcropping accelerograms were then double-integrated to calculate the permanent slope displacement at the ground surface. The 1D numerical analyses were carried out using Shake91 (Schnabel et al., 1972; Idriss and Sun, 1993) while the freeware software by Jibson and Jibson (2003) was used for the Newmark sliding-block calculation.

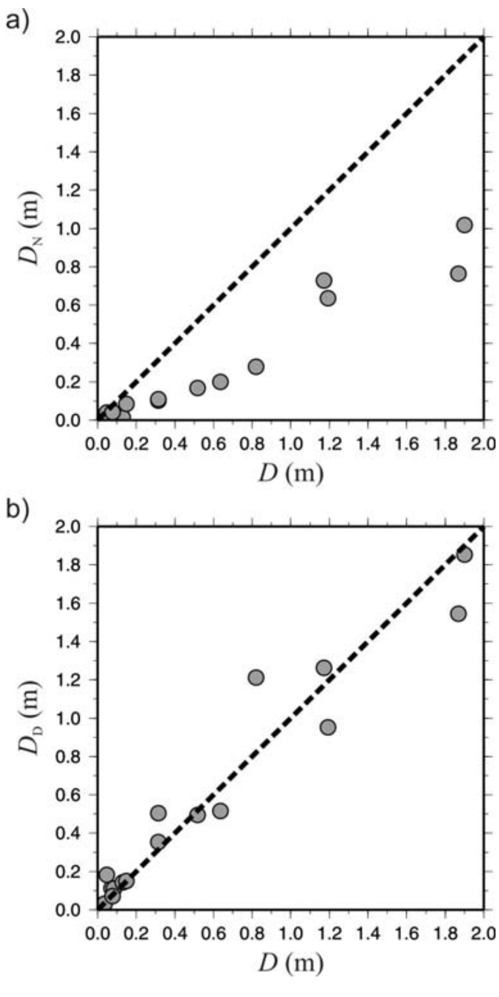

Fig. 8. Comparison of Newmark, D_N,(a) and decoupled D_D, (b) displacements with coupled displacement, D, from 2D analyses.

To determine the slope displacement at the ground surface with the Newmark's method, by applying both the rigid-block and the decoupled assumptions, and to provide a meaningful comparison among the different calculation approaches, we adopted k_y values estimated using Eq. 6 by considering excess pore pressure.

Figure 8 compares Newmark, D_N, decoupled, D_D, and coupled, D, displacements together. Note that D_N and D_D values correspond to the maximum displacement between those calculated by integration of the positive and negative parts of acceleration time histories.

The figure shows that the standard Newmark's sliding-block method severely underestimate the residual displacement. This limitation was of course expected, and it simply confirms that acceleration time histories recorded on rock should not be used to estimate seismic displacements in unstable soil masses. Indeed, except for weak motions, D_N values are significantly lower then those derived from both the decoupled and coupled analyses. These latter approaches, instead, are found to provide similar results. Specifically, the figure shows that decoupled displacements are within about 20% of the coupled results obtained using FLAC.

SEISMIC DISPLACEMENT HAZARD ANALYSIS METHOD

The slope displacement assessment procedure for given level of ground shaking discussed above lends itself into an integration with the conventional seismic hazard analysis at a site. This integration provides an estimate of the annual probability that a displacement of any given amount is experienced at the site where the soil slope is located. The procedure for coupling the slope response with the site hazard has been already presented in previous articles (e.g., Bazzurro et al., 1994; Rathje and Saygili, 2008) and, therefore it will not be repeated here. We only care to discuss here some details that may be important for a correct integration of these two building blocks of the probabilistic slope displacement procedure:

1. Ground motion prediction equations are developed using accelerograms recorded mostly on flat soil. Topographic effects, however, may be altering the amplitude and the frequency content of the ground motion along slopes (e.g., Kramer, 1996). This aspect should be carefully evaluated during computations.

2. If one systematically uses the larger of the two horizontal components of the ground motion coupled with the vertical component to compute the response of a slope, the site hazard should be performed using a prediction equation for the largest of the two horizontal components (e.g., Ambraseys et al., 1996) and not one for the geometric mean, which is the standard parameter predicted in most equations. Neglecting doing so would introduce a bias in the estimate of the annual probability of exceeding slope displacements.

3. If one randomly chooses one of the two horizontal components for the slope assessment then the ground motion prediction equation adopted for the site hazard computations should also use that parameter extracted from an arbitrary component and not the geometric mean from both components. The expected value of the parameter would be identical in both but the uncertainty in the geometric mean case would be smaller than the uncertainty in the arbitrary component case (Baker and Cornell, 2006). If this aspect is neglected, the annual probability of slope displacement would be underestimated.

4. If one uses a standard prediction equation for the geometric mean of a ground motion parameter, then one should use the same geometric mean of the two components during the statistical regression for the slope displacement estimation even if only one horizontal component (and not both) are used (Baker and Cornell, 2006). In other words, the regressions in Figs 5 or 7 should be performed using the geometric mean of the ground motion parameter from both horizontal components.

CONCLUSIONS

This study has presented a probabilistic method for estimating earthquake-induced nonlinear slope displacements for given ground motion scenarios. Precisely, 2D numerical analyses were performed to derive a set of empirical relations for the prediction of soil displacement as a function of one or more ground motion parameters. This soil response function can then be coupled with Probabilistic Seismic Hazard Analysis (PSHA) at the bedrock to establish the annual rate of exceedance of permanent slope deformations of different severity.

The predictive power of several combinations of different ground motion parameters was investigated via regression analysis. Results revealed that the response spectrum intensity is the single most helpful parameter in predicting slope displacement. This confirms results from various authors (e.g., Makdisi and Seed, 1978; Jibson, 1993; Harp and Wilson, 1995) showing that period-independent parameters are well correlated with slope displacement. In particular, our results agree with observations of Makdisi and Seed (1978) and Bray (2007) indicating that the Housner intensity is the most efficient intensity measure for evaluation of the response of flexible slopes with initial fundamental period between 0.6 and 2.0 s. Among period-dependent parameters, the spectral acceleration at the soil fundamental period, $Sa(T_S)$, was found the most informative one. However, if one is prepared to use more than one ground motion parameter (a price that is paid later on in coupling those results with a vectorized version of PSHA rather than its more conventional scalar counterpart), the use of $Sa(T_S)$, in conjunction with the spectral acceleration at a given oscillator period, may yield a lower error in predicting the soil displacements than using any other single ground motion parameter that we investigated here. In particular, for the case study presented in this paper, the use of $Sa(T_S)$ and the spectral acceleration at a period in the neighborhood of 0.25 s, which corresponds approximately to the resonant period of the uppermost soil layer of the landslide mass, was found to improve the prediction. However, this finding cannot be extrapolated to other landslides characterized by different geological and geomorphological settings, and further research is required to investigate the benefit of including the information carried by the resonant periods of shallow soil layers into an empirical model for the prediction of the slope displacements.

As a result of the comparison of slope displacements calculated using alternative approaches, we deduced that the coupled procedure, using the code FLAC, and the decoupled approach, involving 1D site response analyses and subsequent double integration of the computed acceleration time history, can provide similar results provided that the excess pore pressure is properly estimated and considered in the estimate of k_y. On the other hand, the comparison confirmed that slope displacements estimated by double integrating acceleration time histories recorded on rock, without keeping into account site amplification, may severely under-predict the permanent displacement that, in our study, was found to be as much as 50% lower than that provided by the coupled analysis.

ACKNOLEDGMENTS

The authors are grateful to Dr. Roberto De Ferrari (University of Genoa) for providing us Arias intensity values of input motions used in numerical simulations. They are also thankful to Dr. Salvatore Martino (University of Rome, “La Sapienza”) for his helpful suggestions and fruitful discussions about the Salcito landslide modeling.

REFERENCES

Ambraseys, N. N., K. A. Simpson and J. J. Bommer [1996], “Prediction of horizontal response spectra in Europe”, Earthquake Engineering and Structural Dynamics, No. 25, pp. 371-400.

Arias, A [1970], “A measure of earthquake intensity”, in: Seismic design for Nuclear Powerplants, MIT Press, Cambridge (MA), pp. 438-483.

Baker, J.W. and C.A. Cornell [2006], “Which spectral acceleration are you using?”, *Earthquake Spectra*, No. 22, pp. 293-312.

Barani S., R. De Ferrari, G. Ferretti and C. Eva [2010], “Calibration of soil amplification factors for Real-time ground-motion scenarios in Italy”, *submitted for publication on Proc. Fifth International Conference on Recent Advances in Geotechnical Earthquake Engineering and Soil Dynamics.*

Barani, S., R. De Ferrari, G. Ferretti and D. Spallarossa

[2007], "Seismic landslide hazard analysis for the Genoa district, Liguria – Italy", *Proc. 4th International Conference on Earthquake Geotechnical Engineering*, June 25-28, Thessaloniki, Greece, Paper No. 1434.

Bazzurro, P. and C.A. Cornell [2004a], "Ground-motion amplification in nonlinear soil sites with uncertain properties", Bull. Seism. Soc. Am., No. 94, pp. 2090-2109.

Bazzurro, P. and C.A. Cornell [2004b], "Nonlinear soil-site effects in probabilistic seismic-hazard analysis", Bull. Seism. Soc. Am., No. 94, pp. 2110-2123.

Bazzurro, P., and C.A. Cornell [2002], "Vector-valued probabilistic seismic hazard analysis (VPSHA)" *Proc. 7th U.S. National Conf. on Earthquake Engineering*, Vol. II, EERI, Oakland, Calif., pp. 1313-1322.

Bazzurro, P., F. Pelli, G.M. Manfredini and C.A. Cornell [1994], "Stability of sloping seabed: Seismic damage analysis: Methodology and application", Proc. 3rd Symposium on Strait Crossings, June 12-15, Ålesund, Norway, pp. 821-829.

Bianchi Fasani, G., F. Bozzano, C. Esposito, M.R. Manuel, S. Martino, A. Prestininzi and G. Scarascia Mugnozza [2004], "An example of earthquake triggered landslide in structurally complex formations", *Proc. of IX International Symposium on Landslides*, Rio de Janeiro, pp. 321-327.

Bozzano, F., L. Lenti, S. Martino, A. Paciello and G. Scarascia Mugnozza [2008], "Self-excitation process due to local seismic amplification responsible for the reactivation of the Salcito landslide (Italy) on 31 October 2002", J. Geophys. Res., No. 113, B10312, pp. 1-21.

Bozzano, F., S. Martino, G. Naso, A. Prestininzi, R.W. Romeo and G. Scarascia Mugnozza [2004], "The large Salcito landslide triggered by the 31st October 2002, Molise earthquake", Earthquake Spectra, No. 20, pp. 1 -11.

Bray J.D. and T. Travasarou (2007), "Simplified procedure for estimating earthquake-induced deviatoric slope displacements", Journal of Geotechnical and Geoenvironmental Engineering, No. 133, pp. 381-392.

Bray, J.D. [2007], "Simplified slope displacement procedures", *Pitilakis K.D. (ed.), Earthquake Geotechnical Engineering*, pp. 327-353.

Bray, J.D., E.M. Rathje, A.J Augello and S.M. Merry [1998], "Simplified seismic design procedures for geosynthetic-lined, solid waste landfills", Geosynthetics International, No. 5, pp. 203-235.

Comitè Europèen de Normalisation [2003], "prENV 1998-1 – Eurocode 8: Design of structures for earthquake resistance. Part 1: General rules, seismic actions and rules for buildings", Draft No. 4, Brussels, Belgium.

Cundall, P.A., H. Hansteen, S. Lacasse and P.B. Selnes, P.B. [1980], "NESSI – soil structure interaction programme for dynamic and static problems". Report 51508-9, December. Norwegian Geotechnical Institute.

Gruppo di Lavoro CPTI [2004], "Catalogo Parametrico dei Terremoti Italiani, versione 2004 (CPTI04)", INGV, Bologna, http://emidius.mi.ingv.it/CPTI/.

Harp, E.L. and R.C. Wilson [1995], "Shaking intensity thresholds for rock falls and slides: evidence from 1987 Whittier Narrows and Superstition Hills strong-motion records", Bull. Seism. Soc. Am., No. 85, pp. 1739-1757.

Housner, G.W. [1952], "Spectrum intensities of strong motion earthquakes", *Proc. Symposium on earthquake and blast effects on structures*, EERI, Oakland, California, USA, pp. 20-36.

Idriss, I. M. and J.I. Sun [1993], "User's manual for Shake91: A computer program for conducting equivalent linear seismic response analyses of horizontally layered soil deposits", Center for geotechnical modeling, Dept. of Civil and Environmental Engineering, University of California, Davis.

Itasca Consulting Group, Inc. [2005], "FLAC – Fast Lagrangian Analysis of Continua, Version 5.0 User's Manual", Minneapolis: Itasca.

Jibson, R.W. [1993], "Predicting earthquake-induced landslide displacements using Newmark's sliding block analysis", Transportation Research Board, Transportation Research Record 1411, pp. 9-17.

Jibson, R.W. [2007], "Regression models for estimating coseismic landslide displacement", Engineering Geology, No. 91, pp. 208-218.

Jibson, R.W. and M.W. Jibson [2003]. "Java programs for using Newmark's method and simplified decoupled analysis to model slope performance during earthquakes", US Geological Survey Open-File Report 03-005.

Kramer, S. L. [1996], "*Geotechnical earthquake engineering*, Prentice-Hall, New Jersey".

Kuhlemeyer, R.L. and J. Lysmer [1973], "Finite element method accuracy for wave propagation problems", Journal of Soil Mechanics and Foundations, No. 99, pp. 421–427.

Lin, J.-S. and R.V. Whitman [1983], "Decoupling approximation to the evaluation of earthquake-induced plastic slip in earth dams", Earthquake Engrg. and Struct. Dyn., No. 11, pp. 667-678.

Lysmer, J. and R.L. Kuhlemeyer [1969], "Finite dynamic model for infinite media", Journal of Engineering Mechanics, No. 95, pp. 859–877.

Makdisi, F.I. and H.B. Seed [1978], "Simplified procedure for estimating dam and embankment earthquake-induced deformations", J. Geotech. Engrg. Div., No. 104, pp. 849-867.

Mejia, L.H. and E.M. Dawson [2006], "Earthquake Deconvolution for FLAC", *Proc. 4th International FLAC Symposium*, Madrid, Spain, pp. 211-219.

Miles, S.B. and C.L Ho [1999] "Rigorous landslide hazard zonation using Newmark's method and stochastic ground motion simulation", Soil Dynamics and Earthquake Engineering, No. 18, pp. 305-323.

Ministero delle Infrastrutture e dei Trasporti [2008], "Norme tecniche per le costruzioni – NTC, D.M. 14 Gennaio 2008", Supplemento ordinario alla Gazzetta Ufficiale No 29, 4 Febbraio 2008.

Newmark, N.M. [1965], "Effects of earthquakes on dams and embankments", Geotechnique, No. 15-2, pp. 139-160.

Rathje E.M. and J.D. Bray [2000], "Nonlinear coupled seismic sliding analysis of earth structures", Journal of Geotechnical and Geoenvironmental Engineering, No. 126, pp. 1002-1014.

Rathje L.M. and G. Saygili [2008], "Probabilistic seismic hazard analysis for the sliding displacement of slopes: scalar and vector approaches", Journal of Geotechnical and Geoenvironmental Engineering, No. 134, pp. 804-814.

Romeo, R. [2000], "Seismically induced landslide displacements: a predictive model", Engineering Geology, No. 58, pp. 337-351.

Schnabel, P.B., J. Lysmer and H.B. Seed [1972], "SHAKE: a computer program for earthquake response analysis of horizontally layered sites", Report No. UCB/EERC-72/12, Earthquake Engineering Research Center, University of California, Berkeley, 92p.

Stucchi, M., R. Camassi, A. Rovida, M. Locati, E. Ercolani, C. Meletti, P. Migliavacca, F. Bernardini and R. Azzaro [2007]. "DBMI04, il database delle osservazioni macrosismiche dei terremoti italiani utilizzate per la compilazione del catalogo parametrico CPTI04", Quaderni di Geofisica, No. 49, 38 pp., http://emidius.mi.ingv.it/DBMI04/.

Travasarou, T. and J.D. Bray [2003], "Optimal ground-motion intensity measures for assessment of seismic slope displacements", Pacific Conference on Earthquake Engineering, Christchurch, New Zealand.

Wartman, J., J.D. Bray and R.B. Seed [2003], "Inclined plane studies of the Newmark sliding block procedure", Journal of Geotechnical and Geoenvironmental Engineering, No. 129, pp. 673-684.